Materials Horizons

COMMUNICATION

View Article Online
View Journal

CrossMark click for updates

Cite this: DOI: 10.1039/c6mh00568c

Received 8th December 2016,
Accepted 13th January 2017

DOI: 10.1039/c6mh00568c

rsc.li/materials-horizons

A flexible p-CuO/n-MoS_2 heterojunction photodetector with enhanced photoresponse by the piezo-phototronic effect†

Ke Zhang,‡[a] Mingzeng Peng,‡[a] Wei Wu,[a] Junmeng Guo,[a] Guoyun Gao,[a] Yudong Liu,[a] Jinzong Kou,[a] Rongmei Wen,[a] Ying Lei,[a] Aifang Yu,[a] Yang Zhang,[a] Junyi Zhai*[a] and Zhong Lin Wang*[ab]

Flexible functional devices based on two dimensional (2D) materials are extremely suitable for malleable, portable and sustainable applications, such as health monitoring, electronic skin and optoelectronics. In this work, we developed a flexible photodetector based on a p-CuO/n-MoS_2 heterojunction with an enhancement in photocurrent and detection sensitivity. Because of the non-centrosymmetric structure in monolayer MoS_2, the piezo-potential induced by applied strain adjusts the band structure at the heterojunction interface and broadens the depletion region based on the piezo-phototronic effect. The border depletion can be discreetly used to improve the photo-generated carrier separation and transport to enhance photoresponse performance. When illuminated by a 532 nm laser, the photocurrent of the heterojunction can be enhanced 27 times under a tensile strain of 0.65% compared to strain free conditions and the detection sensitivity can reach up to 3.27 × 10^8 Jones. As a result, our research provides a new strategy for novel design and performance optimization of 2D material heterostructures in the application of optoelectronics.

Conceptual insights

Transition metal dichalcogenide (TMD) material based optoelectronic devices have been developed rapidly due to their excellent visible light response and ultra-fast photovoltaic conversion. We demonstrate that applied strain can further dramatically tune the optoelectronic properties in TMD p–n junctions owing to piezo-phototronics, while most of the previous studies have avoided or reduced the impact of strain dependent properties. The largest piezoelectric effect in monolayer MoS_2 is in-plane and occurs along the Mo–S bond orientation, which can easily be identified by the triangle shape of CVD-grown MoS_2. When strain is applied to MoS_2 along the Mo–S bond direction, piezo-charge will be induced and control the carrier generation, transport, separation and/or recombination at the interface of p-CuO/n-MoS_2, improving the performance of optoelectronic devices. As a result, both the photo-induced current and sensitivity of the pn junction based photodetector are largely enhanced. This method provides a new strategy to improve the optoelectronic properties in TMD based pn junctions by applying strain.

Introduction

Transition metal dichalcogenides (TMDCs) have recently emerged as a new class of semiconductor materials of electronics and optoelectronics.[1,2] Molybdenum disulfide (MoS_2), the representative of TMDCs, not only has a 1.8 eV direct band gap for the monolayer, which is superior to that of graphene (zero gap), but also has other advantages such as good stability and brilliant optoelectronic properties.[2–4] However, most photodetectors,[5,6] phototransistors,[7] solar cells[8,9] and other optoelectronic devices with excellent performance based on monolayer MoS_2 are often fabricated on hard substrates (silicon wafer, sapphire, *etc.*). 2D materials, owing to their outstanding ductility and high mechanical strength,[10] are well adapted for flexible optoelectronic devices in new application fields, such as biomedical diagnosis, personal health monitoring and wearable communication.[11–13] However, it is challenging to achieve a better performance on polymer-based flexible substrates due to inevitable substrate strain, the limitation of transferring methods and complex fabrication. Among them, for flexible optoelectronics, strain from a flexible substrate has a large influence on the device performance, due to the piezoresistive effect, stress concentration and stress softening. Although there were a few reports[14,15] of TMD based flexible devices in the last several years, they avoided or reduced the impact of strain as far as possible. Our study aims at applying the inevitable substrate strain to improve the performance of photodetectors based on the strong piezoelectric effect in monolayer MoS_2.

[a] *Beijing Institute of Nanoenergy and Nanosystems, Chinese Academy of Science, National Center for Nanoscience and Technology (NCNST), Beijing 100083, P. R. China. E-mail: jyzhai@binn.cas.cn, zlwang@gatech.edu*

[b] *School of Materials Science and Engineering, Georgia Institute of Technology, Atlanta, Georgia 30332-0245, USA*

† Electronic supplementary information (ESI) available. See DOI: 10.1039/c6mh00568c

‡ These authors contributed equally to this work.

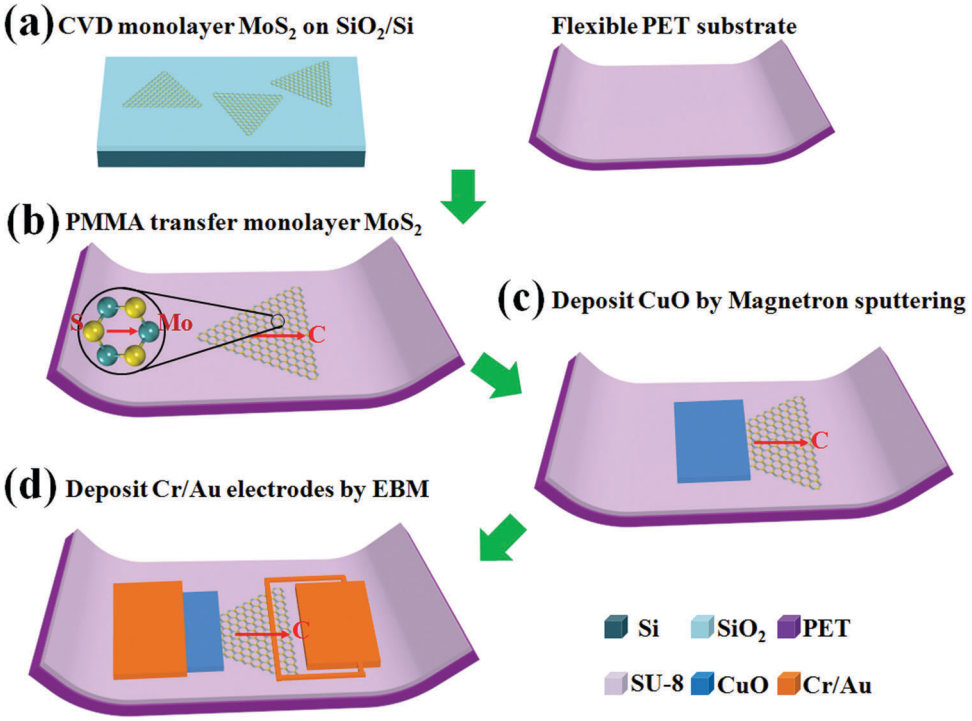

Fig. 1 Fabrication flowchart of the flexible p-CuO/n-MoS_2 heterojunction photodetector. (a) Monolayer MoS_2 grown on the SiO_2/Si substrate and flexible PET substrate with a layer of SU-8. (b) Transferring MoS_2 to the PET substrate using a PMMA-assisted method. (c) Using magnetron sputtering to deposit a layer of CuO film on defined areas exposed by EBL. (d) Depositing Cr/Au (10/100 nm) electrodes by EBM.

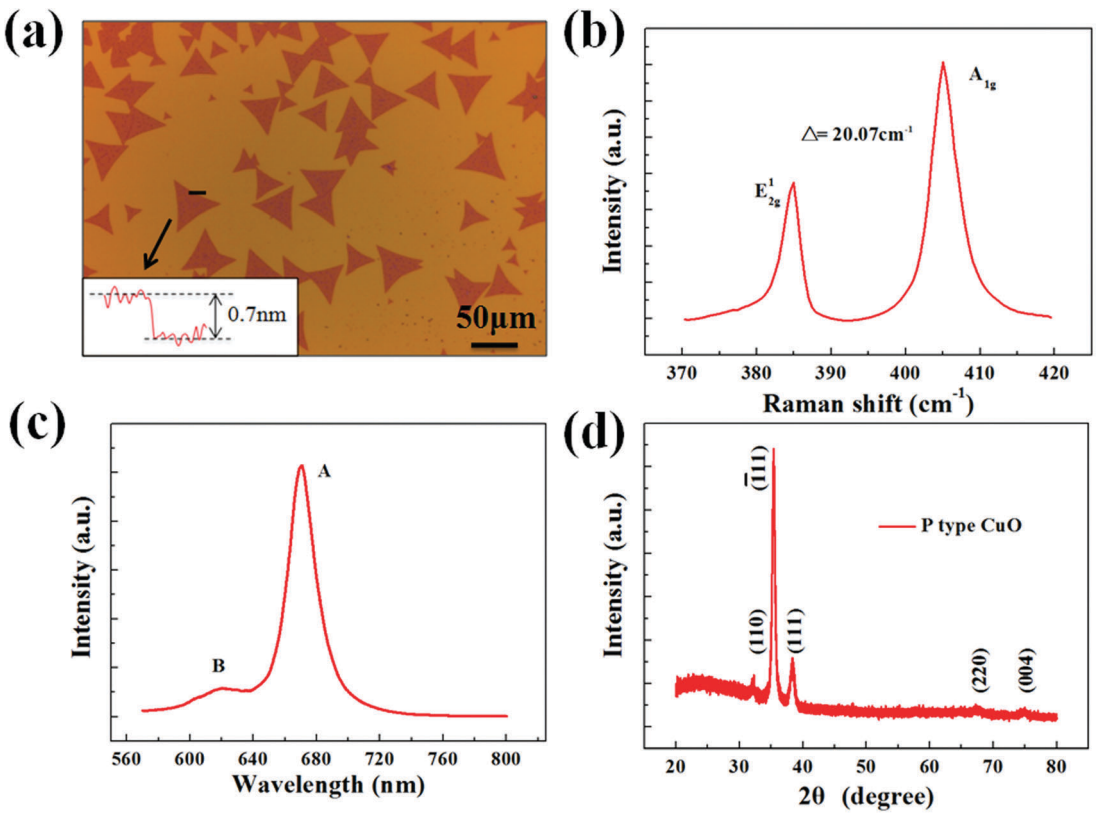

Fig. 2 The characterization of monolayer MoS_2 and p-type CuO. (a) Optical reflection image of CVD growth of a typical triangle monolayer MoS_2 on the SiO_2/Si substrate. The inset shows the thickness of MoS_2 is $\approx$0.7 nm which is measured by AFM. (b) The Raman spectrum of the CVD grown MoS_2 on the SiO_2/Si substrate. The frequency separation between E^1_{2g} and A_{1g} peaks is 20.07 cm^{-1} MoS_2. The excitation laser is 532 nm. (c) The photoluminescence spectrum of the CVD grown monolayer MoS_2. The excitation laser is 532 nm. (d) The XRD spectrum of p-type CuO film deposited by magnetron sputtering.

Recently, a piezoelectric effect in MoS_2 with an odd number of atomic layers was reported which could be used to modulate the height of the schottky barrier in metal-semiconductor contacts and/or power nano-devices owing to its non-centrosymmetric structure[13,16] Moreover, it is easy to identify the Mo–S bond orientation (direction with a strongest piezoelectric effect) from the triangular single-layer CVD grown MoS_2.[17,18] Meanwhile, the piezo-phototronic effect is to use the piezopotential to control the carrier generation, transport, separation and/or recombination for improving the performance of optoelectronic devices, such as photodetectors, solar cells, LEDs and pressure-sensitive photoluminescence imaging.[19–23] Although the piezo-phototronic effect has been well studied in wurtzite ZnO or GaN nanowire based LEDs, solar cells and photodetectors, there is still a lack of research on how piezopotential tunes the photoelectric properties in a monolayer 2D material based heterostructure.[24,25]

In this study, we developed a flexible p-CuO/n-MoS_2 heterojunction photodetector to obtain high optoelectronic performance by the piezo-phototronic effect. High quality triangular monolayer n-type MoS_2 grown by chemical vapor deposition (CVD) was used to form a p–n heterojunction with a p-type CuO film deposited by magnetron sputter deposition. Under the external stimuli, the piezopotential induced by piezoelectric charges at the side of the monolayer MoS_2 adjusted the band structure at the interface of the heterojunction and separated the photogenerated electron–hole pairs more effectively to increase the photocurrent. In addition, the structure of the p–n junction can also reduce the screening effect from a lot of free electrons in n-type materials and depress the dark current in order to get larger photoresponsivity and higher detection sensitivity. Our flexible photodetector based on p-CuO/n-MoS_2 gave an ultra-low dark current of 0.039 nA and a detection sensitivity of 3.27×10^8 Jones. The results demonstrate that the piezo-phototronic effect has potential for improving the performance of electronics and optoelectronics based on 2D materials and related heterostructures, especially for flexible sensing applications.

Results and discussion

The fabrication process of the flexible CuO–MoS_2 heterojunction device is illustrated in Fig. 1. MoS_2 monolayers were firstly grown on silicon wafers with a 300 nm thick silica layer (SiO_2/Si) by chemical vapor deposition (CVD), as described in previous studies.[18,26] Secondly, an SU-8 photoresist was spin-coated on a PET substrate to get a relatively flat and smooth surface. After spin-coating, the PET substrate was baked at 135 °C for two hours. Thirdly, the monolayer CVD-grown MoS_2 was transferred to the PET substrate by using polymethylmethacrylane (PMMA) as shown in Fig. 1b.[27,28] Fourthly, a

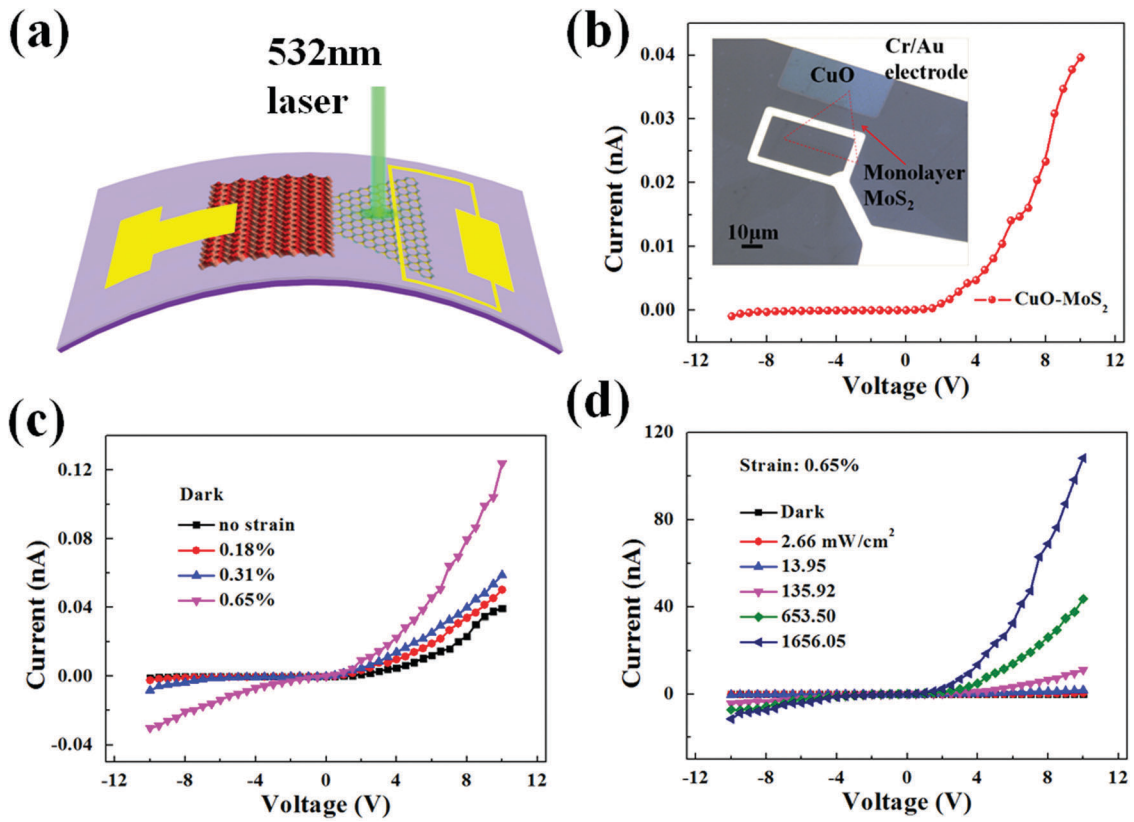

Fig. 3 (a) Schematic diagram of the flexible photodetector based on the p-CuO/n-MoS_2 heterojunction. (b) *I–V* curve of the p-CuO/n-MoS_2 heterojunction in the dark and in a strain free state. The inset is the optical image of the device. (c) *I–V* curves of the heterojunction in the dark with increasing tensile strain. (d) *I–V* curves measured at 0.65% tensile strain and different illumination light powers. All curves were measured at room temperature and in the air. A 532 nm laser was used to excite the photocurrent.

PMMA electron beam resist was spun on the PET substrate and a specific area was exposed by electron beam lithography. Fifthly, a 150 nm thick p-type CuO film was deposited by magnetron sputtering to form a p–n junction with MoS_2. Finally, Cr/Au (10 nm/100 nm) electrodes were deposited on both sides of the p-CuO/n-MoS_2 heterojunction by electron beam lithography (EBL) and electron beam evaporation deposition (EBM) (Fig. 1c and d). In detail, the polarity orientation (*C* axis) of the CVD-grown MoS_2 from the S to Mo atom with a strongest piezoelectric effect was indicated by the red arrow as shown in Fig. 1e. In order to investigate the performance modulation of the piezoelectric effect, both the rectangle p-type CuO film and Cr/Au electrodes were deposited perpendicular to the *C* axis of MoS_2.

Fig. 2a shows the surface morphology of the CVD grown triangle MoS_2 on the SiO_2/Si substrate using an optical microscope. The typical side length ranges from 40 to 70 μm. Besides, the thickness of the MoS_2 flakes is around 0.7 nm, measured by atomic force microscopy (AFM), which approaches the theoretical thickness of monolayer MoS_2.[29] Raman and photoluminescence (PL) spectra of the CVD-grown monolayer MoS_2 flakes are presented in Fig. 2b and c, respectively. The energy difference between its A_{1g} (405.02 cm^{-1}) and E^1_{2g} (384.95 cm^{-1}) Raman modes is 20.07 cm^{-1}, confirming that the MoS_2 flakes are monolayers.[30,31] The PL spectrum consists of two peaks at 670 nm (1.85 eV) and 620 nm (2.00 eV), corresponding to the A and B direct gap optical transition.[32] P-type CuO film was fabricated by a standard magnetron sputter deposition using a high purity Cu target and Ar/O_2 (1 : 4) sputtering gases at room temperature. It has excellent quality further proved by the XRD spectrum (Fig. 2d).[33,34]

The structure of the flexible p-CuO/n-MoS_2 heterojunction photodetector is demonstrated in Fig. 3a. We used a 532 nm laser (facula diameter is about 3 μm), to illuminate the side of MoS_2 and avoid the photoresponse influence from the p-CuO layer. A high precision manual translation table was used to bend the PET substrate. By this means, well controlled strain can be applied to the monolayer MoS_2, as shown in Fig. S1 (ESI†). Moreover, we examined the photoresponse of the pure p-CuO film in different tensile strain states and at various optical power densities (Fig. S2a and S2b, ESI†). The results indicate that the photoresponse of CuO in the scope of illumination power is very small and can be omitted comparing to the performance of the p–n heterojunction device. The photoresponse of pure monolayer MoS_2 is also studied and the device just performs the piezoresistive effect (Fig. S2c and S2d, ESI†). Next, the *I–V* characteristics of the p-CuO/n-MoS_2 heterojunction were investigated with various illumination power densities and strains. Fig. 3b shows good rectification characteristics of the p-CuO/n-MoS_2 heterojunction under dark and strain free conditions. It had an ultra-low dark current of 0.039 nA even under 10 V forward bias, which was advantageous for high performance optical sensing. The relationship of the photogenerated current with different strains in the dark is presented in Fig. 3c.

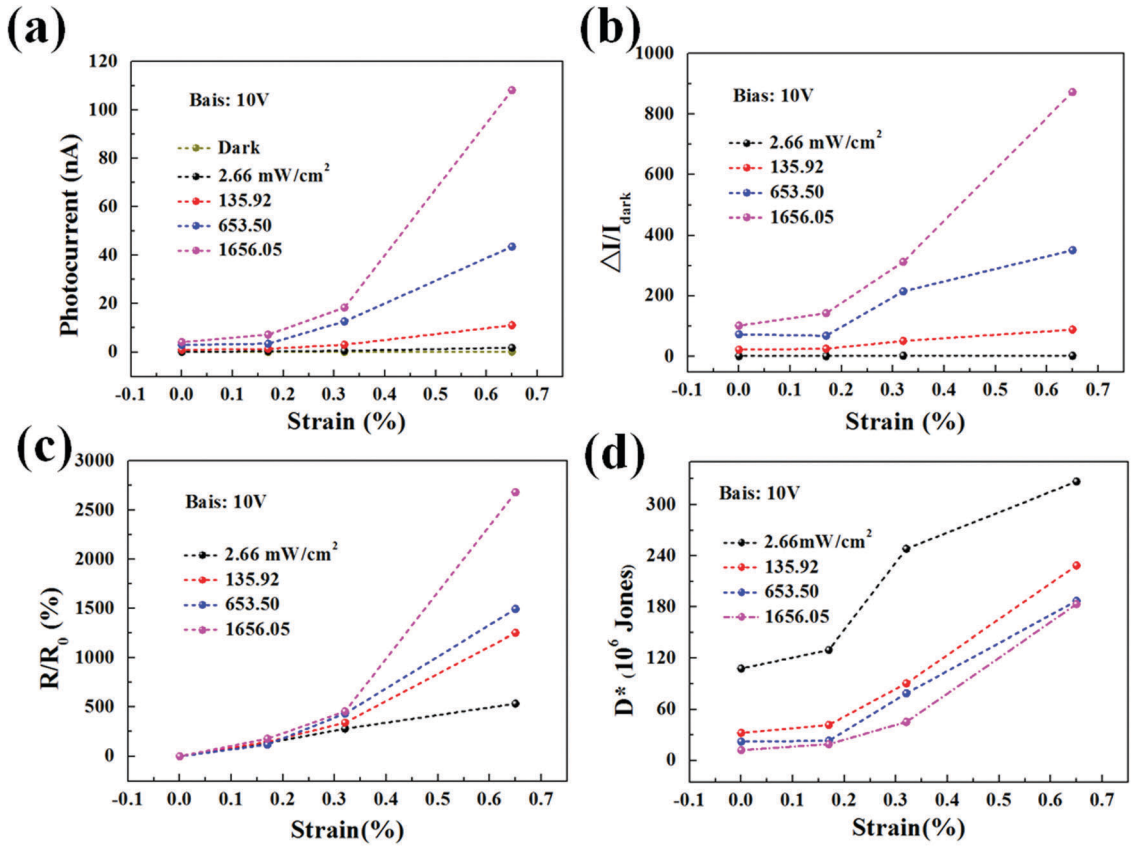

Fig. 4 The strain dependence of the (a) photocurrent, (b) $\Delta I/I_{dark}$, (c) R/R_0 and (d) detectivity (D^*) at different power densities at a bias of 10 V.

The dark current under 10 V bias increases from 0.039 nA to 0.12 nA with increasing tensile strain from 0% to 0.65%. This is mainly attributed to the piezotronic effect of single layer MoS_2 (positive piezopotential induced by tensile strain tunes the bandgap at the heterojunction interface of CuO and MoS_2). In order to further investigate the influence of the piezo-phototronic effect on the p-CuO/n-MoS_2 heterojunction performance, we tested the *I–V* characteristic with increasing illumination power density from dark to 1656 mW cm^{-2} and tensile strain from 0% to 0.65%. The photocurrent is always enhanced with the increasing of either the luminous power or tensile strain. The photocurrent of the p–n heterojunction device can reach to the maximum value of 108 nA under 1656 mW cm^{-2} illumination and 0.65% tensile strain, which is about a 2770 times improvement in current output compared to its dark current in a strain free state. Meanwhile, the time-dependent photoresponse of the device to periodical on/off illumination under different tensile strains is shown in Fig. S3 (ESI†). The device has excellent stability under various strains over a long time period.

According to the *I–V* characteristics of the p-CuO/n-MoS_2 heterojunction photodetector, we evaluated the photocurrent (I_{ph}), photosensitivity ($\Delta I/I_{dark}$), relative changes in photoresponsivity (R/R_0), and detectivity (D^*) under different illumination intensities (0 mW cm^{-2} (dark), 2.66 mW cm^{-2}, 135.92 mW cm^{-2}, 653.50 mW cm^{-2}, 1656.05 mW cm^{-2}) and tensile strains (0%, 0.18%, 0.31%, 0.65%), as summarized in Fig. 4. The relationship of photocurrent I_{ph} with different tensile strains under various power densities is shown in Fig. 4a. Under the 532 nm laser illumination, the photocurrent increases with the increasing of strain due to the piezo-phototronic effect. When the illumination power is fixed at 1656.05 mW cm^{-2}, the photocurrent I_{ph} is enhanced 27 times under a strain of 0.65% compared with strain-free conditions. To demonstrate its photoresponse mechanism clearly, the photosensitivity is calculated using the formula $\Delta I/I_{dark} = (I_{light} - I_{dark})/I_{dark}$, where the I_{light} and I_{dark} are the output current with and without illumination under a certain external strain, respectively. Meanwhile, the relative change in responsivity is defined as R/R_0 (R_0 is the corresponding R under strain-free conditions) for different power densities. It can be seen that the relationships of $\Delta I/I_{dark}$ and R/R_0 with tensile strain have a similar manner as photocurrent I_{ph} under different illumination powers in Fig. 4b and c. The maximum values of $\Delta I/I_{dark}$ and R/R_0 are 873 and 2680% respectively, achieved at the highest tensile strain of 0.65% and light power of 1656.05 mW cm^{-2}, owing to the piezo-phototronic effect on modulating energy and the structure at the interface of CuO/MoS_2. Moreover, we show the photoresponsivity of our photodetector in Fig. S4 (ESI†), which also increases with the increasing of strain due to the piezo-phototronic effect. The detectivity under different strains is calculated using formula the $D^* = R/(2eI_{dark}/S)^{0.5}$, where e is the

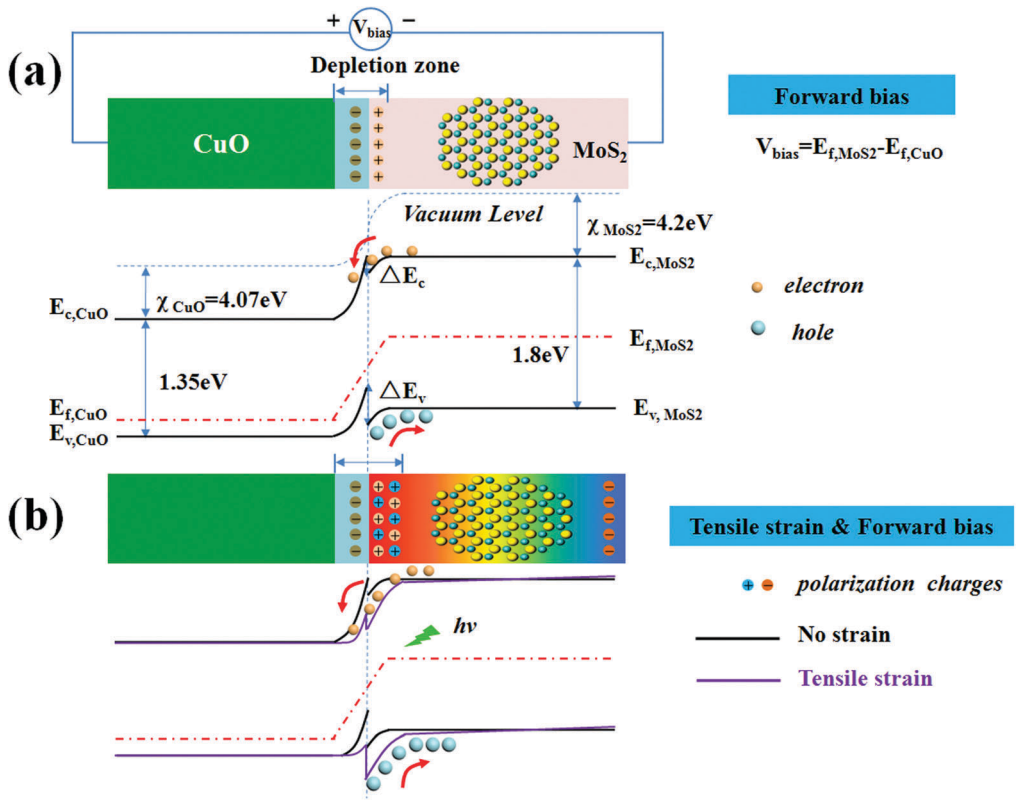

Fig. 5 (a) Band diagram of the p-CuO/n-MoS_2 heterojunction in the equilibrium state with forward bias. ΔE_c = 0.13 eV, ΔE_v = 0.68 eV. (b) Band diagram with forward-bias voltage in a strain free state (black line) and tensile strain state (purple line). When tensile strain is applied, the induced positive piezoelectric polarization charges at the interface will cause a decline for the band edge (purple line) and increase the width of the depletion zone. For the color gradient, red represents positive potential and blue represents negative potential.

quantity of electric charge, I_{dark} is dark current and S is the effective surface area of the CuO/MoS_2 heterojunction photodetector. We found that D^* reaches the highest value of 3.27×10^8 Jones under the highest strain of 0.65% and lower light power of 2.66 mW cm^{-2} in Fig. 4d.

In order to elucidate the intrinsic mechanism of piezo-phototronics for modulating the photoresponse performance of the p-CuO/n-MoS_2 heterojunction, its band structures of the heterojunction with/without tensile strain have been compared. Fig. 5a shows its band diagrams under strain-free and forward bias conditions. The electron affinity and band gap of p-CuO are 4.07 eV and 1.35 eV, respectively[35] while the monolayer MoS_2 has 4.2 eV electron affinity and 1.8 eV direct band gap.[36] Therefore, a conduction band offset ΔE_c = 0.13 eV and a valence band offset ΔE_v = 0.68 eV present at local heterostructure interface. The electrons and holes flow towards CuO and MoS_2 respectively because of the joint action of built-in electric field and external forward bias. Under the laser irradiation of 532 nm (2.33 eV), the photo-generated electron–hole pairs are separated by a built-in field, producing external photocurrent. When tensile strain is applied to the flexible device, monolayer MoS_2 generates the mechanical deformation and produces positive piezoelectric charges at the heterostructure interface due to the piezotronic effect. As a result, the positive piezopotential induced by polarization charges enhances the conduction band and valence band energy level bending of MoS_2 near the interface and the depletion zone is broadened at the same time. At the interface of CuO/MoS_2, both stronger electric field and the expanded depletion zone provide an extra driving force to separate photo-generated electrons and holes more efficiently. Meanwhile, it also reduces the recombination of photogenerated electron–hole pairs, accelerates the transportation of carriers and increases photocurrent. Therefore, under the forward bias, the photocurrent increases a lot mainly because of the piezo-phototronic effect (Fig. 5b). Of course, the piezoresistive effect can also cause an increase of photocurrent, but it is considered as the ''volume effect'' and has an equivalent change in the device performance under either dark or illumination conditions, as shown in Fig. S2d (ESI†). However, our experimental results manifest that the performance of the photodetector has more enhancement by applying tensile strain in illumination than that in the dark. In summary, the piezo-phototronic effect plays a major role in the photoresponse enhancement of the p-CuO/n-MoS_2 photodetector.

Conclusions

In summary, we successfully fabricated a flexible and high-performance p-CuO/n-MoS_2 heterojunction based photodetector. We take advantage of the unique characteristics in CVD-grown monolayer MoS_2, such as a strong piezoelectric effect and simple determination of polarity direction, to optimize the optoelectronic performance of flexible detectors by applied strain. Based on the piezo-phototronic effect, the piezopotential induced by monolayer MoS_2 under strain conditions has dramatically adjusted the band structure in the interface of the monolayer MoS_2-based heterojunction and separated photogenerated electron–hole pairs more effectively to increase the device photocurrent. Here, the flexible p-CuO/n-MoS_2 photodetector under 0.65% tensile strain has up to 27 times improvement in responsivity compared to strain-free conditions with a detection sensitivity of 3.27×10^8 Jones in low light illumination. Due to the ultra-flexibility and high mechanical strength of 2D materials, TMDCs (MoS_2, WSe_2, $MoTe_2$, *etc.*) with the piezoelectric effect will be more competitive for nanoelectronic devices for applications in flexible sensors and ultrathin optoelectronics.

Methods

Growth procedure and transfer of MoS_2

Monolayer MoS_2 was grown on 300 nm thick SiO_2/Si substrates by chemical vapor deposition. A quartz boat containing 15 mg MoO_3 powder ($\geq$99.5%, Sigma Aldrich), which served as a precursor, was positioned in the center of a furnace and the Si substrate was placed face down in the boat above the precursor. 270 mg sulfur ($\geq$99.9%, Aladdin) was located outside of the furnace, warmed up by heating tape. The furnace temperature was increased up to 750 °C at a rate of 15 °C min^{-1} and held constant for 30 minutes at this point, and then cooled down naturally. When the furnace temperature reached 650 °C, the heating tape started working. The growth was carried on under atmospheric pressure with 10 sccm argon flow.

During the transfer process, a thin layer of PMMA (495 K, A11, MicroChem) was spun coated firstly on the CVD grown MoS_2, and then baked for 3 minutes at 150 °C. Next, the sample coated by PMMA was floated on 30% HF solution to etch SiO_2. Finally, the detached film was cleaned in deionized water several times and transferred to the target substrate.

Author contribution

The manuscript was written through contributions of all authors. All authors have given approval to the final version of the manuscript. K. Z., J. Y. Z and Z. L. W conceived the idea. K. Z. and J. M. G. prepared the materials. K. Z., W. W., and G. Y. G. fabricated the devices. K. Z., M. Z. P. and Y. D. L. conducted the electrical test. J. Z. K, R. M. W., Y. L., A. F. Y., and Y. Z performed the material characterization. K. Z. and M. Z. P. analyzed the data and wrote the manuscript instructed by J. Y. Z. and Z. L. W. with input from all the authors.

Acknowledgements

This work was supported by NSFC 51472056 and 51402064, the ''thousands talents'' program for pioneer researcher and his innovation team, China, the Recruitment Program of Global Youth Experts, China, Youth Innovation Promotion Association of Chinese Academy of Sciences (2015387) and The National Key Research and Development Program of China (2016YFA0202703).

Notes and references

1 S. Das, J. A. Robinson, M. Dubey, H. Terrones and M. Terrones, *Annu. Rev. Mater. Res.*, 2015, **45**, 1–27.
2 Q. H. Wang, K. Kalantar-Zadeh, A. Kis, J. N. Coleman and M. S. Strano, *Nat. Nanotechnol.*, 2012, **7**, 699–712.
3 K. F. Mak, C. Lee, J. Hone, J. Shan and T. F. Heinz, *Phy. Rev. Lett.*, 2010, **105**, 136805.
4 A. K. Geim and K. S. Novoselov, *Nat. Mater.*, 2007, **6**, 183–191.
5 C. Chen, H. Qiao, S. Lin, C. Man Luk, Y. Liu, Z. Xu, J. Song, Y. Xue, D. Li, J. Yuan, W. Yu, C. Pan, S. Ping Lau and Q. Bao, *Sci. rep.*, 2015, **5**, 11830.
6 O. Lopez-Sanchez, D. Lembke, M. Kayci, A. Radenovic and A. Kis, *Nat Nanotechnol.*, 2013, **8**, 497–501.
7 W. Choi, M. Y. Cho, A. Konar, J. H. Lee, G.-B. Cha, S. C. Hong, S. Kim, J. Kim, D. Jena, J. Joo and S. Kim, *Adv. Mater.*, 2012, **24**, 5832–5836.
8 S. Lin, X. Li, P. Wang, Z. Xu, S. Zhang, H. Zhong, Z. Wu, W. Xu and H. Chen, *Sci. Rep.*, 2015, **5**, 15103.
9 M.-L. Tsai, S.-H. Su, J.-K. Chang, D.-S. Tsai, C.-H. Chen, C.-I. Wu, L.-J. Li, L.-J. Chen and J.-H. He, *ACS Nano*, 2014, **8**, 8317–8322.
10 S. Bertolazzi, J. Brivio and A. Kis, *ACS Nano*, 2011, **5**, 9703–9709.
11 D. Ruh, P. Reith, S. Sherman, M. Theodor, J. Ruhhammer, A. Seifert and H. Zappe, *Adv. Mater.*, 2014, **26**, 1706–1710.
12 D. Akinwande, N. Petrone and J. Hone, *Nat. Commun.*, 2014, **5**, 5678.
13 W. Wu, L. Wang, Y. Li, F. Zhang, L. Lin, S. Niu, D. Chenet, X. Zhang, Y. Hao, T. F. Heinz, J. Hone and Z. L. Wang, *Nature*, 2014, **514**, 470–474.
14 M.-Y. Tsai, A. Tarasov, Z. R. Hesabi, H. Taghinejad, P. M. Campbell, C. A. Joiner, A. Adibi and E. M. Vogel, *ACS Appl. Mater. Interfaces*, 2015, **7**, 12850–12855.
15 J. Pu, Y. Yomogida, K.-K. Liu, L.-J. Li, Y. Iwasa and T. Takenobu, *Nano Lett.*, 2012, **12**, 4013–4017.
16 H. Zhu, Y. Wang, J. Xiao, M. Liu, S. Xiong, Z. J. Wong, Z. Ye, Y. Ye, X. Yin and X. Zhang, *Nat. Nanotechnol.*, 2015, **10**, 151–155.
17 S. K. Kim, R. Bhatia, T.-H. Kim, D. Seol, J. H. Kim, H. Kim, W. Seung, Y. Kim, Y. H. Lee and S.-W. Kim, *Nano Energy*, 2016, **22**, 483–489.
18 A. M. van der Zande, P. Y. Huang, D. A. Chenet, T. C. Berkelbach, Y. You, G.-H. Lee, T. F. Heinz, D. R. Reichman, D. A. Muller and J. C. Hone, *Nat. Mater.*, 2013, **12**, 554–561.
19 W. Wu and Z. L. Wang, *Nat. Rev. Mater.*, 2016, **1**, 16031.
20 W. Wu, L. Wang, R. Yu, Y. Liu, S.-H. Wei, J. Hone and Z. L. Wang, *Adv. Mater.*, 2016, **28**, 8463–8468.
21 M. Peng, Z. Li, C. Liu, Q. Zheng, X. Shi, M. Song, Y. Zhang, S. Du, J. Zhai and Z. L. Wang, *ACS Nano*, 2015, **9**, 3143–3150.
22 W. Wu, C. Pan, Y. Zhang, X. Wen and Z. L. Wang, *Nano Today*, 2013, **8**, 619–642.
23 Z. L. Wang and W. Wu, *Natl. Sci. Rev.*, 2014, **1**, 62–90.
24 M. Peng, Y. Liu, A. Yu, Y. Zhang, C. Liu, J. Liu, W. Wu, K. Zhang, X. Shi, J. Kou, J. Zhai and Z. L. Wang, *ACS Nano*, 2016, **10**, 1572–1579.
25 C. Liu, M. Peng, A. Yu, J. Liu, M. Song, Y. Zhang and J. Zhai, *Nano Energy*, 2016, **26**, 417–424.
26 S. Wang, Y. Rong, Y. Fan, M. Pacios, H. Bhaskaran, K. He and J. H. Warner, *Chem. Mater.*, 2014, **26**, 6371–6379.
27 G. A. Salvatore, N. Münzenrieder, C. Barraud, L. Petti, C. Zysset, L. Büthe, K. Ensslin and G. Tröster, *ACS Nano*, 2013, **7**, 8809–8815.
28 C. R. Dean, A. F. Young, I. Meric, C. Lee, L. Wang, S. Sorgenfrei, K. Watanabe, T. Taniguchi, P. Kim, K. L. Shepard and J. Hone, *Nat. Nanotechnol.*, 2010, **5**, 722–726.
29 B. Radisavljevic, A. Radenovic, J. Brivio, V. Giacometti and A. Kis, *Nat. Nanotechnol.*, 2011, **6**, 147–150.
30 M. Buscema, G. A. Steele, H. S. J. van der Zant and A. Castellanos-Gomez, *Nano Res.*, 2014, **7**, 561–571.
31 H. Li, Q. Zhang, C. C. R. Yap, B. K. Tay, T. H. T. Edwin, A. Olivier and D. Baillargeat, *Adv. Funct. Mater.*, 2012, **22**, 1385–1390.
32 A. Splendiani, L. Sun, Y. Zhang, T. Li, J. Kim, C.-Y. Chim, G. Galli and F. Wang, *Nano Lett.*, 2010, **10**, 1271–1275.
33 C. Liu, A. Yu, M. Peng, M. Song, W. Liu, Y. Zhang and J. Zhai, *J. Phys. Chem. C*, 2016, **120**, 6971–6977.
34 B. Zhao, P. Liu, H. Zhuang, Z. Jiao, T. Fang, W. Xu, B. Lu and Y. Jiang, *J. Mater. Chem. A*, 2013, **1**, 367–373.
35 A. Zainelabdin, S. Zaman, G. Amin, O. Nur and M. Willander, *Appl. Phys. A: Mater. Sci. Process*, 2012, **108**, 921–928.
36 S. Bertolazzi, D. Krasnozhon and A. Kis, *ACS Nano*, 2013, **7**, 3246–3252.